

Research Article

Low Energy Consumption Synthesis of Nanostructured TiO₂ Particles by Combining Oxidant Peroxide Method and Microwave-Assisted Hydrothermal Treatment

A. P. Garcia,^{1,2} I. C. L. Rocha,¹ P. H. F. dos Santos,¹ T. M. Basegio,¹ M. B. Pereira,³
F. J. Clemens,² A. K. Alves,¹ and C. P. Bergmann¹

¹Laboratório de Materiais Cerâmicos, UFRGS, 90035190 Porto Alegre, RS, Brazil

²Laboratory for High Performance Ceramics, EMPA, 8600 Dübendorf, Switzerland

³Laboratório Laser & Óptica, UFRGS, 91501970 Porto Alegre, RS, Brazil

Correspondence should be addressed to A. P. Garcia; anapquimica@yahoo.com.br

Received 21 February 2016; Accepted 21 March 2016

Academic Editor: Donglu Shi

Copyright © 2016 A. P. Garcia et al. This is an open access article distributed under the Creative Commons Attribution License, which permits unrestricted use, distribution, and reproduction in any medium, provided the original work is properly cited.

Titanium dioxide with high specific surface area in the crystalline anatase phase is a promising material for environmental applications. In this work, TiO₂ with good applicability for photocatalytic processes has been obtained using the low energy consumption synthesis based on oxidant peroxide method combined with microwave-assisted low temperature hydrothermal treatment. To prepare the material, titanium propoxide, hydrogen peroxide, and isopropyl alcohol were used. The influence of time and temperature during the hydrothermal step on properties like morphology, crystallinity, phase composition, specific surface area, and photocatalytic behavior were investigated. Photoactivity was measured using the methyl orange decomposition method in UV-A light. Increasing temperature during hydrothermal step, photocatalytic properties could be improved. The nanostructured TiO₂ particles synthesized at 200°C and 30 min with this method showed photocatalytic activity comparable to commercial Aeroxide® TiO₂ P25.

1. Introduction

Titanium dioxide (TiO₂) is a widely used material in heterogeneous photocatalysis because of its unique properties. It is nontoxic, water-insoluble, and resistant to photocorrosion while offering high oxidative power at a low cost [1, 2]. It is also a very promising semiconductor for use in the photodegradation of organic compounds. The band gap of this oxide ranges from 3.0 to 3.2 eV and it can be activated by sunlight [3, 4]. Recently, many studies have focused on obtaining nanostructured products using inexpensive methods, especially those involving lower energy consumption [5]. Several methods, especially those using wet-chemical routes, are widely employed in the synthesis of nanostructured TiO₂ [1]. Studies show that most wet-chemical routes can present some disadvantages: the appearance of secondary phases, nonstoichiometric compositions, and impurities in

the primary products [6]. In this context, combining the oxidant peroxide method (OPM) [7–10] with hydrothermal microwave treatment [11] is an excellent synthesis route to obtain materials with extensive applicability in photocatalysis, such as TiO₂. Use of microwave heating instead of the usual autoclave reactor in the hydrothermal treatment significantly decreases energy consumption during synthesis [12]. This is because the microwave-assisted treatment requires lower temperatures and very short reaction times (in the range of minutes) [13]. The OPM route has received considerable attention because pure and homogeneous powders can be prepared using this method [4]. In this paper we present a simple process to produce nanostructured TiO₂ particles with low energy consumption combining OPM route and microwave-assisted hydrothermal treatment. It was found that the TiO₂ obtained using this combined method was highly suitable for photocatalytic processes.

2. Materials and Methods

2.1. Synthesis. Nanoparticles of TiO_2 were synthesized following an adaptation of the route described by Chang and coworkers [1]. Titanium propoxide (98%, Sigma Aldrich, USA) was used as the titanium source. In a typical experiment, 3 mL titanium propoxide was added to 15 mL isopropyl alcohol (99.5%, Nuclear, Brazil). The mixture was homogenized by stirring (~ 5 min) and 10 mL hydrogen peroxide (35 wt% aqueous solution, Dinamica, Brazil) was added dropwise. The resultant solution was placed in an ice bath for 3 h and finally annealed at three different times (30, 60, and 120 min) and temperatures (100, 150, and 200°C) in a closed-vessel microwave digestion/extraction system (MDS-8G, Sineo, China). Precipitates were washed with isopropyl alcohol (150 mL), filtered, and dried at 50°C for 24 h. Finally, the obtained powders were ground and sieved (#325 mesh).

2.2. Powder Characterization. Crystalline phases and crystallite sizes were characterized by X-ray diffraction (XRD) with a Philips X'pert MPD diffractometer using $\text{CuK}\alpha$ radiation ($\lambda = 0.1541$ nm) operating at 40 kV and 40 mA. The average crystallite size of the samples was estimated by (101) reflection for the anatase phase using the Scherrer equation. To determine the particle primary size, the samples were characterized by transmission electronic microscopy (TEM) using a microscope from JEOL (JEM 2010 TEM, Japan). In this case, the Image Tool® software was used to measure the primary particle size of at least 35 particles for each TEM image examined. Morphology of the samples was investigated employing scanning electron microscopy (SEM) using a JEOL JSM-6060 SEM (Japan) operating at 20 kV. The evaluation of mass loss as a function of temperature (thermal gravimetric analysis, TGA) was performed in a synthetic air atmosphere and a heating rate of $10^\circ\text{C min}^{-1}$ up to 1000°C (SDT Q600, TA Instruments, USA). To determine the specific surface area (S_{BET}) by Brunauer-Emmett-Teller (BET) theory, Autosorb Quantachrome Instrument (NOVA 1000, USA) and N_2 gas were used. The UV-Vis diffuse reflectance was measured using a Cary 5000 spectrophotometer (Agilent, USA) equipped with a DRA-1800 Integrating Sphere. The band gap energies were calculated using the Kubelka-Munk function [14].

2.3. Photocatalytic Characterization. Methyl orange dye (analytical grade, Sigma Aldrich, USA) was used as the model compound for photocatalytic measurements. In these tests, 100 mg of each sample was added to 100 mL of a 20 mg L^{-1} dye solution. This mixture was ultrasonically homogenized in a dark chamber for 16 min. This procedure was adopted to improve the dispersion of the mixture. The dye solution and catalyst were placed into a Pyrex reactor under constant magnetic stirring and temperature (thermostatted water bath at 30°C). The mixture was exposed to compressed air flow and UV-A radiation from 8-W black light lamps (Fluor BLB T5, Sadokin, Brazil). An aliquot of the suspension (~ 5 mL) was collected immediately after homogenization (dark chamber) and every 15 min after starting irradiation. Color disappearance was monitored using the Cary 7000

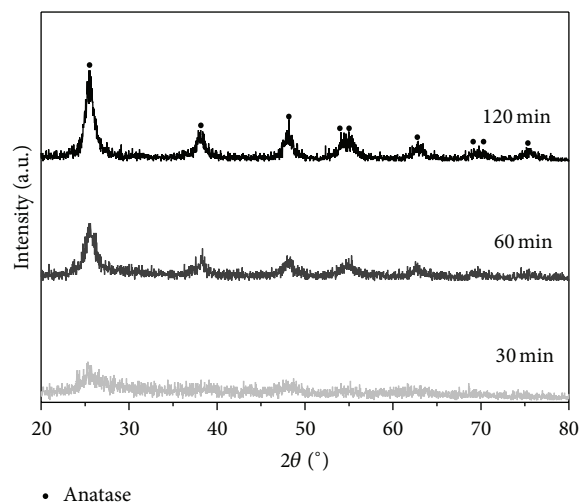


FIGURE 1: X-ray diffraction patterns of samples obtained at 100°C.

at 465 nm (Agilent, USA). The adsorption and photolysis tests were also performed in which the same conditions were used except for the presence of UV radiation and catalyst, respectively. For comparison, the commercial product Aeroxide TiO_2 P25 (Evonik, Germany) was used. All experiments were performed in triplicate to achieve reliable photocatalytic behavior for the comparison.

3. Results and Discussion

Chemical phase analyses by XRD measurement are shown in Figures 1 and 2. Samples prepared at 100°C (Figure 1) had a broad baseline in each diffractogram, indicating the presence of large quantities of an amorphous phase. The anatase phase (PDF 01-0562) was confirmed in XRD patterns of TiO_2 prepared using at least 60 min of hydrothermal treatment for samples treated at this temperature. Because some OPM products require low calcination temperatures for achieving pure phase materials [4], the amorphous powders may be readily converted into crystalline products without use of large amounts of energy. Based on that, we emphasize that the diffraction peak in the XRD curves of samples prepared at 100°C for 30 min is already slightly visible in the background and it can be strategically used to produce materials to determined applications with low energy consumption.

Peaks for the anatase phase (PDF 01-0562) were observed in the XRD patterns for all samples prepared at 150°C and 200°C (Figures 2(a) and 2(b)). For samples prepared at 150°C the amorphous phase is still higher in comparison with synthesized samples at 200°C. It is assumed that crystallinity increases even between 150 and 200°C. Anatase TiO_2 with a good degree of crystallization can be synthesized using microwave irradiation at 200°C even at 30 min of microwave irradiation. The crystallinity of TiO_2 synthesized in this work by OPM and microwave-assisted hydrothermal treatment at 200°C is much higher than crystallinity of TiO_2 obtained in previous work without microwave irradiation [1].

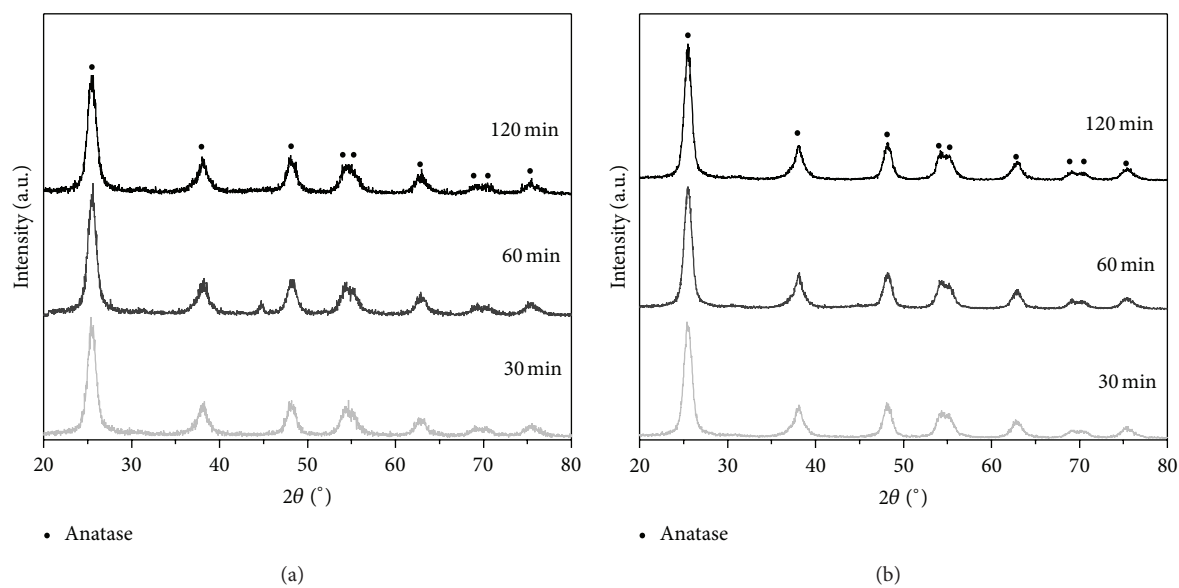


FIGURE 2: X-ray diffraction patterns of samples obtained at (a) 150°C and (b) 200°C.

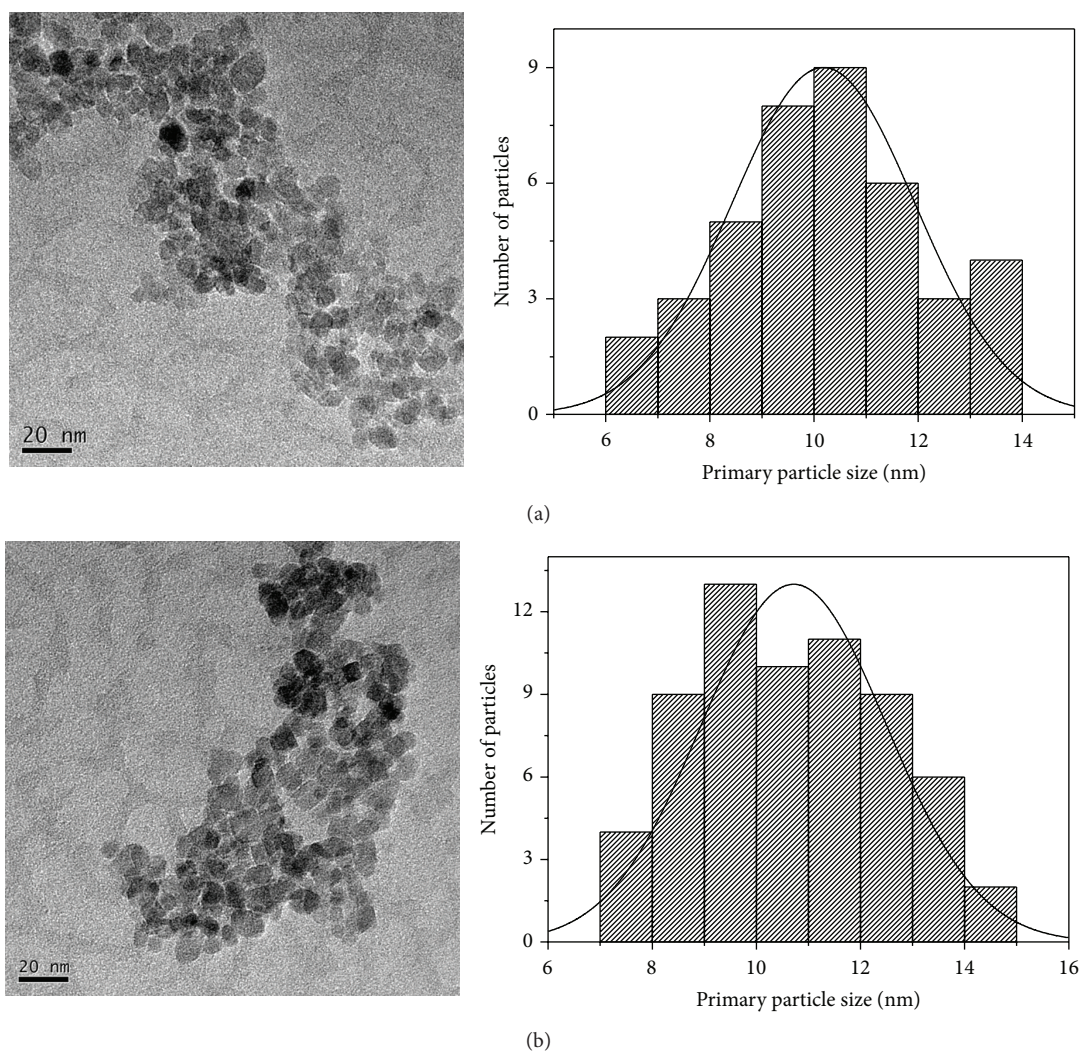


FIGURE 3: TEM images and primary particle size distributions of samples prepared at (a) 150°C and (b) 200°C for 30 min under microwave irradiation.

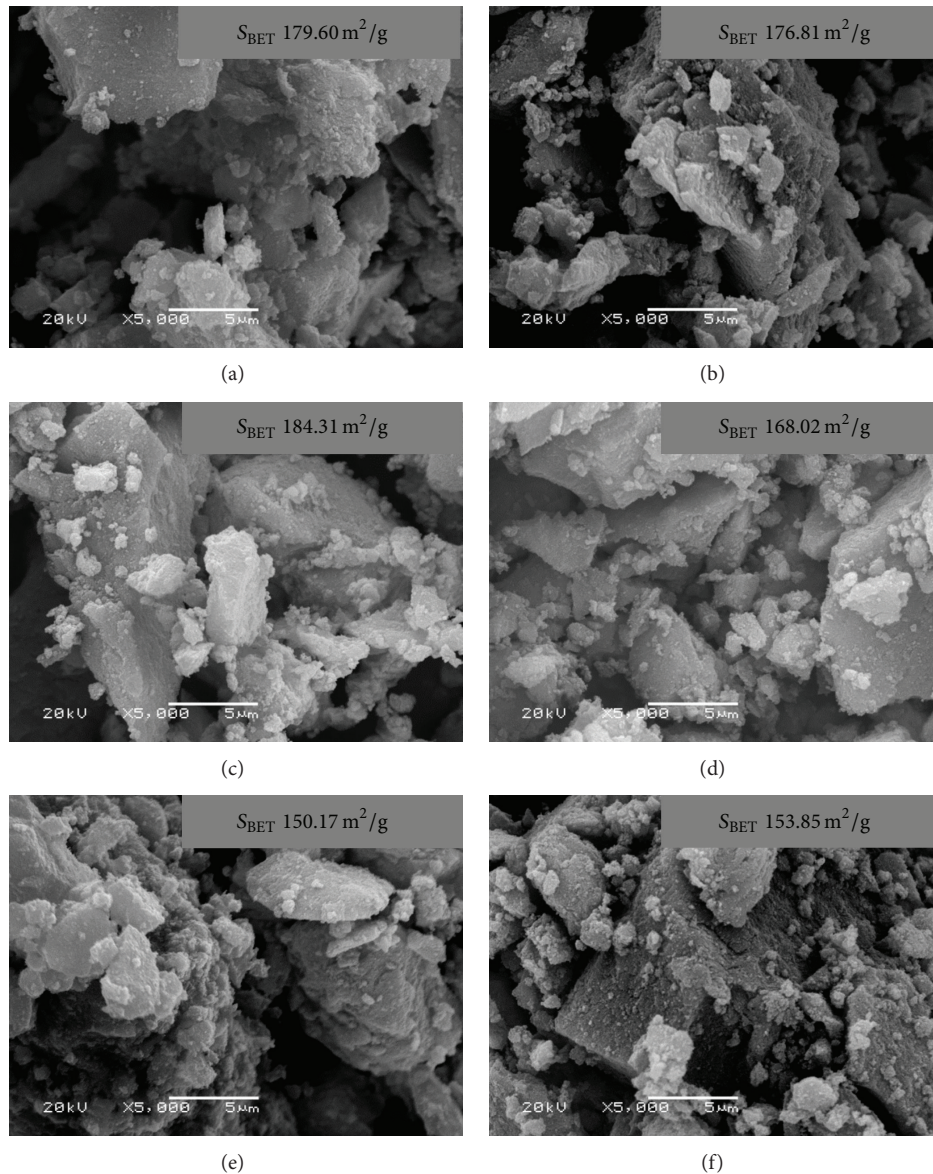


FIGURE 4: SEM images and S_{BET} areas of samples obtained at 150°C ((a) 30 min, (b) 60 min, and (c) 120 min) and 200°C ((d) 30 min, (e) 60 min, and (f) 120 min).

In this case, TiO_2 powders were prepared using OPM route without microwave irradiation and required 24 h reaction time. Jiang et al. [11] concluded that the synthesis of a single and homogeneous anatase phase is completely achievable by adjusting the temperature and time in a microwave system. They observed that peak intensities in XRD patterns narrowed gradually with increasing time and/or temperature of hydrothermal exposure, in good agreement with our results. The production of anatase TiO_2 at low temperatures by a friendly green method represents environmental gain. Wang et al. [15] proposed that the crystallization of TiO_2 produced by OPM is related to the vigorous exothermic decomposition that occurs during synthesis. Using the OPM route, all organic compounds are probably degraded after the

heating process, resulting from the exothermic reaction in the synthesis stage. Consequently, the densification and crystallization steps can occur at lower temperatures without further difficulties. The average crystallite and primary particle sizes are given in Table 1. The TEM images (Figures 3(a) and 3(b)) reveal that samples particles obtained at both temperatures are spherical in shape and range in size between 5 and 15 nm. Mean primary particle sizes, according to TEM histograms, were about 10.2 and 10.7 nm for samples produced at 150°C and 200°C, respectively.

Formation of particle agglomerations, independent of synthesis temperature, was also observed. Sample morphology in SEM images with the respective specific surface area is shown in Figure 4. The samples show similar aggregated

TABLE 1: Average crystallite and primary particle size of TiO₂ samples in this work.

Synthesis parameters		Crystallite size (nm) Scherrer equation	Primary particle size (nm) TEM
150°C	30 min	5.7	10.2
	60 min	6.0	9.9
	120 min	5.9	8.8
200°C	30 min	6.3	10.7
	60 min	6.4	10.0
	120 min	6.9	10.8

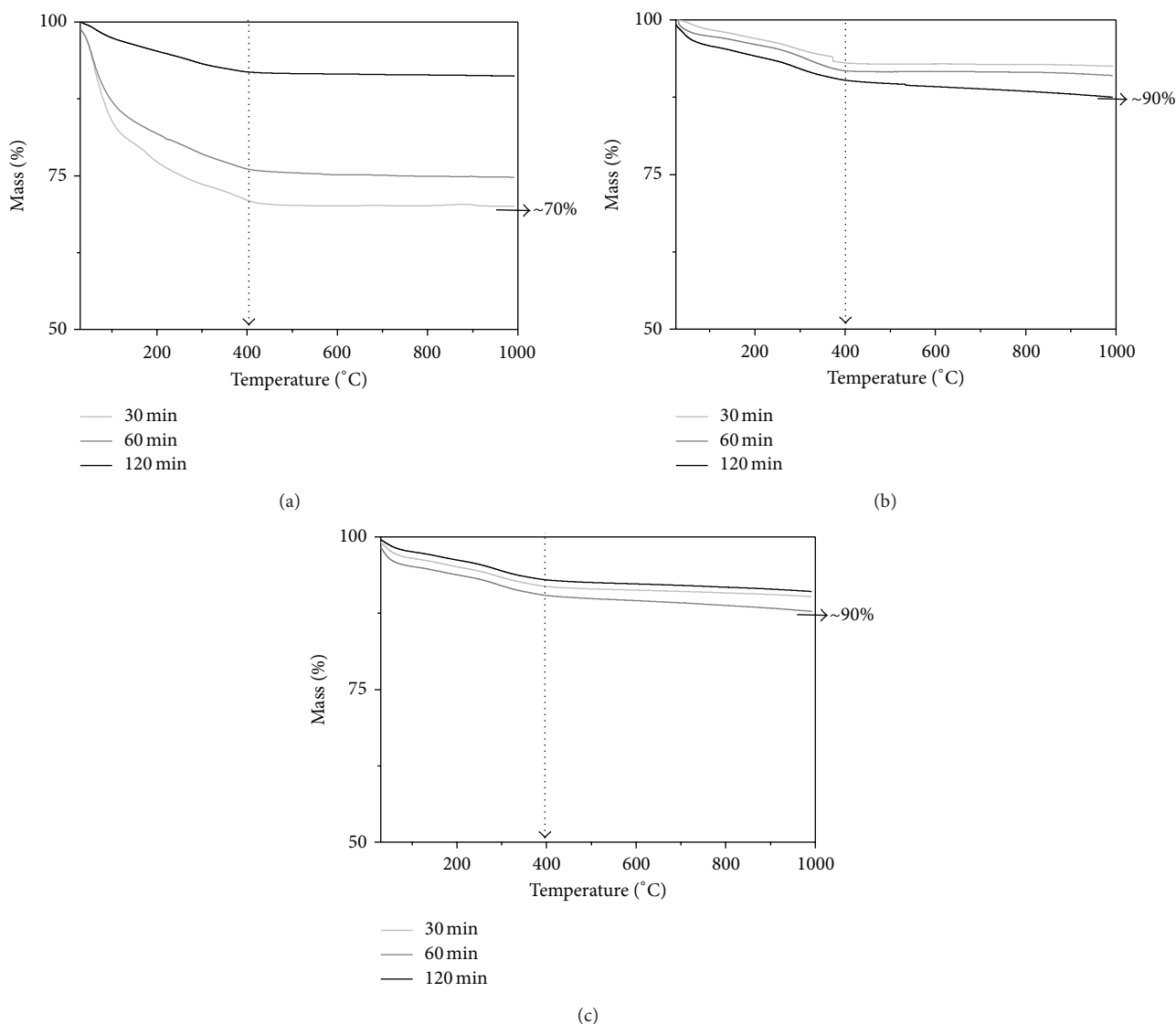


FIGURE 5: Thermogravimetric curves of the obtained samples at (a) 100°C, (b) 150°C, and (c) 200°C.

morphology structure. Apparently, hydrothermal time had no significant effect on the specific surface areas at any temperature investigated.

The thermogravimetric analyses are present in Figure 5. Maximum mass loss (~30%) was observed in samples obtained using 30 min of hydrothermal treatment at 100°C, as

shown in Figure 5(a). According to the literature, the weight loss observed in a temperature range up to 400°C (dotted line) is attributed to the removal of hydration water and OH surface groups of TiO₂. This also may be associated with some unreacted alkoxy groups since organic precursors like titanium propoxide and isopropyl alcohol in the synthesis

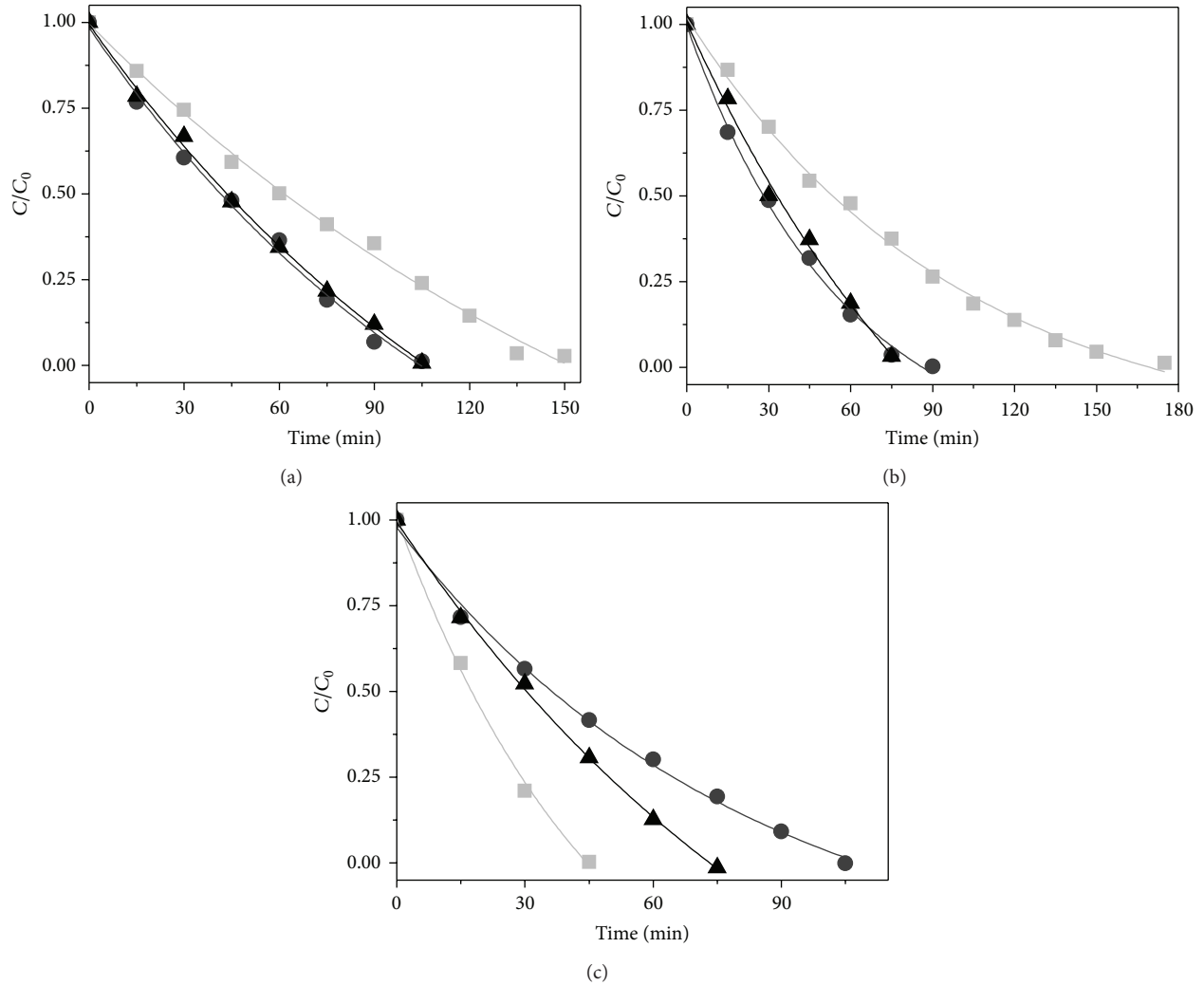


FIGURE 6: Photocatalytic activity of TiO₂ powders prepared at 150°C with (a) 30 min, (b) 60 min, and (c) 120 min of hydrothermal treatment.

reactions were used [16]. These results might be explained by the burning of remaining peroxy groups and organic compounds not totally decomposed in the exothermic stage (peroxytitanate complex formation) [14]. As a matter of fact, the processed powders prepared during 30 and 60 min at 100°C have intense yellow color which is characteristic of the presence of the chemical bond between titanium and hydrogen peroxide [17]. Total mass losses for samples prepared at 150°C and 200°C (Figures 5(b) and 5(c)) were relatively low and, in both cases, close to 10%, which is probably associated with the evaporation of absorbed water [18].

The band gap energy and adsorption band were investigated for the samples synthesized at 150 and 200°C (Table 2). It can be observed that neither temperature nor exposure time has an influence on the band gap energy of nanostructured TiO₂. The results are consistent with that reported by Yu et al. [19]. He explained this by the similarity of the surface microstructure and chemical phase composition. It is important to mention that the band gap energy for TiO₂ produced

TABLE 2: Band gap energy (eV) and absorption band (λ) of TiO₂ samples.

Synthesis parameters	λ (nm)	E_g (eV)
150°C	30 min	376
	60 min	376
	120 min	365
200°C	30 min	365
	60 min	365
	120 min	365

in this way is very close to 3.2 eV, the characteristic band gap of this oxide [3].

In the absence of photocatalysts or UV light irradiation the concentration of methyl orange after 120 min of experiment decreased 5 and 15%, respectively. However, the predominant phenomenon responsible for the color disappearance was the photocatalytic degradation, as shown

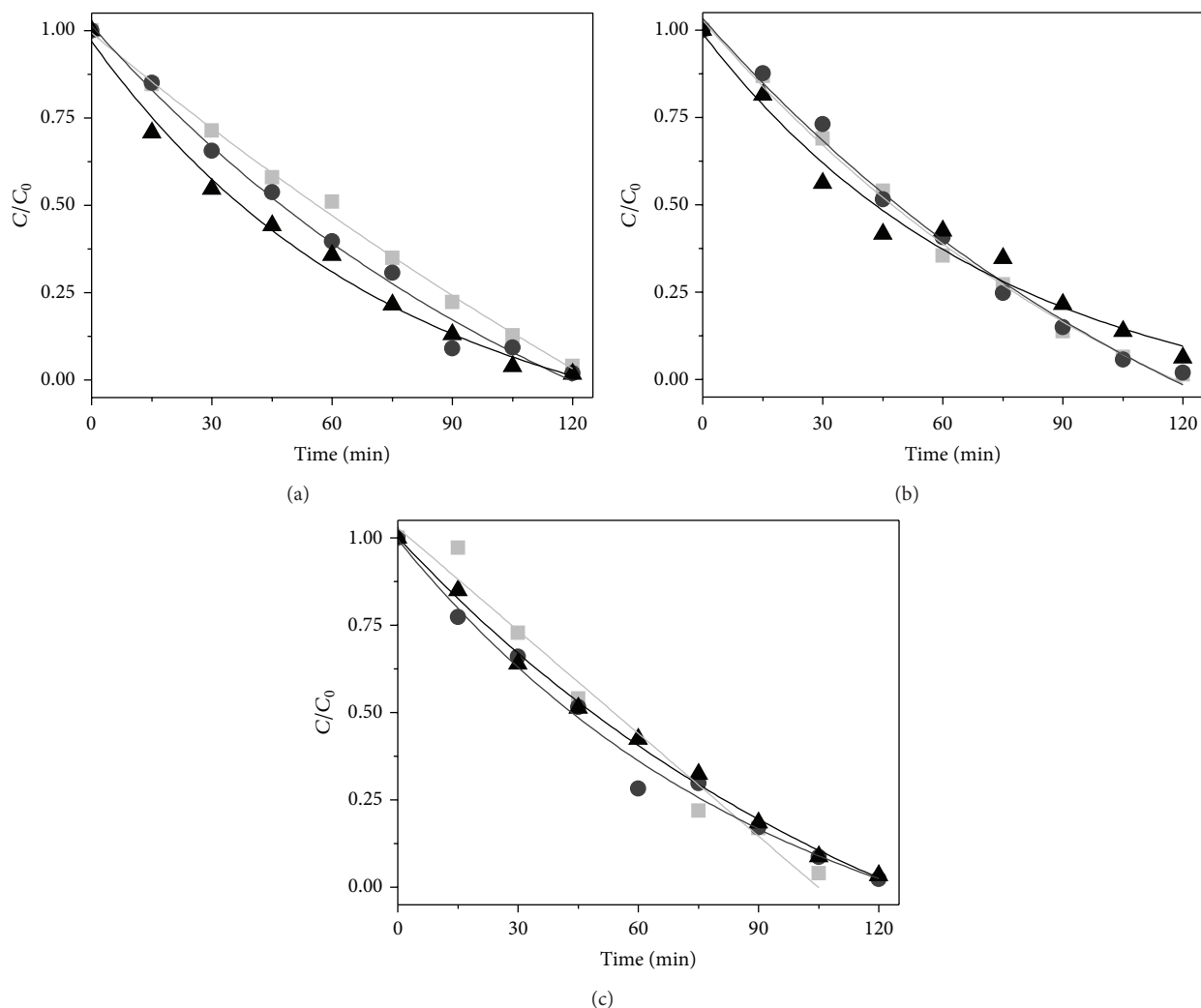


FIGURE 7: Photocatalytic activity of TiO₂ powders prepared at 200°C with (a) 30 min, (b) 60 min, and (c) 120 min of hydrothermal treatment.

below. Interestingly the decomposition of methyl orange dye is affected by the synthesis temperature (Figures 6 and 7). The degradation curves of methyl orange obtained for the samples prepared at 150°C and 200°C can be seen in Figures 6 and 7, respectively. For the samples synthesized at 150°C a large variation in the photocatalytic activity can be observed among the replicates with the same material.

This can be attributed to the fact that the energy associated with this temperature may not have been sufficient to convert all precursors into crystalline products and amorphous phase is still present, which may be explained by the fact that amorphous titania has low or no significant photocatalytic activity. In this case, the recombination of e^- and h^+ is facilitated by the defects located on the surface and in the bulk of the particles of noncrystalline materials [20]. The variation of the photocatalytic behavior for samples synthesized at 200°C is much smaller (Figure 7). According to the results shown in Figure 7, the exposure time has no significant influence on the photocatalytic behavior of TiO₂ synthesized at 200°C.

The main idea of this study was the development of a photocatalytic material with low energy consumption during synthesis step. Samples synthesized at 200°C and 30 min were compared with the photocatalytic performances of P25 (Figure 8).

It can be seen that samples obtained by OPM and microwave-assisted hydrothermal treatment at 200°C and commercial P25 powder present comparable catalytic activity on dye degradation. Peaks for the anatase (PDF 01-073-1764) and rutile (PDF 01-088-1172) phases were observed in the XRD pattern of TiO₂ P25 as shown in Figure 9. Beside the fact that previous reports have indicated a mixed-phase TiO₂ as a good combination for photocatalytic applications [21, 22], it was possible to reach an equivalent degradation performance using pure anatase TiO₂ catalyst in this work. On the other hand, these results are in agreement with other studies that relate the anatase phase as being suitable for photocatalytic systems due to its unique characteristics [23, 24]. These results are remarkable because of the low energy consumption preparation method: only organic-metallic compounds and low temperatures were employed.

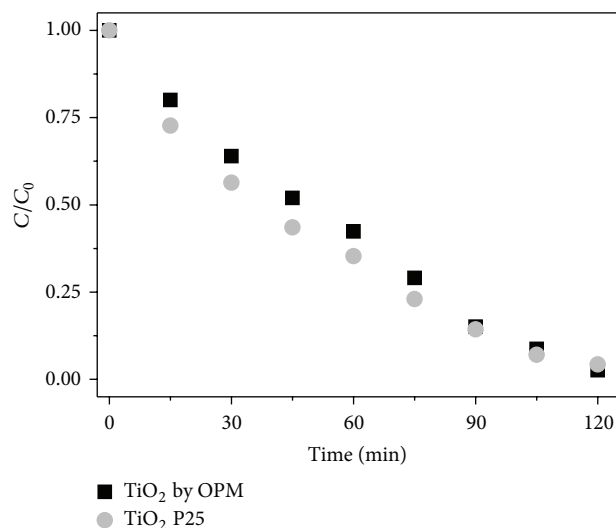


FIGURE 8: Photocatalytic activity of TiO₂: commercial product (P25) and a sample prepared at 200°C with 30 min of microwave hydrothermal treatment.

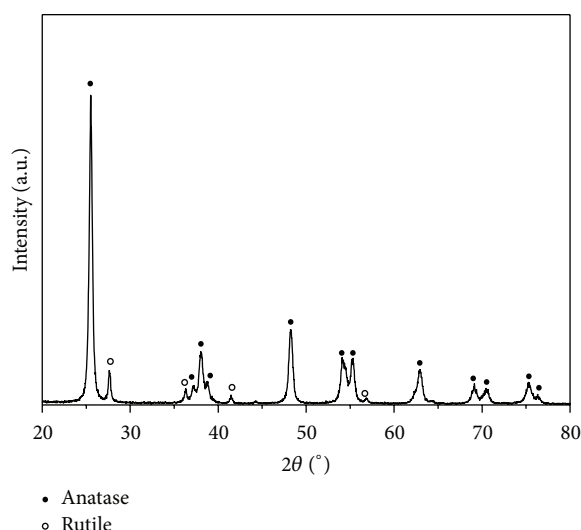


FIGURE 9: X-ray diffraction pattern of TiO₂ P25.

Furthermore, calcination or doping was not necessary to achieve such performance, since the as-prepared catalysts exhibited good photocatalytic activity on removal of pollutants from water as the methyl orange.

4. Conclusions

Nanostructured TiO₂ can be prepared using a combination of OPM and a microwave-assisted hydrothermal treatment. Highly photoreactive anatase nanostructured TiO₂ particles were obtained at 200°C. According to TEM analysis, mean primary particle sizes were around 10.2 and 10.7 nm for synthesis at 150°C and 200°C during 30 min, respectively. The band gap energies were quite similar regardless of synthesis parameters and were in the range of 3.3 to 3.4 eV. However

the particles prepared at 200°C displayed homogeneous photocatalytic activities. These photocatalytic activities are comparable with commercial product, Aeroxide TiO₂ P25. The low energy consumption synthesis process presented in this work represents a gain for the environment because no posterior heat treatment (calcination) or doping of nanostructured TiO₂ particles was required.

Competing Interests

The authors declare that they have no competing interests.

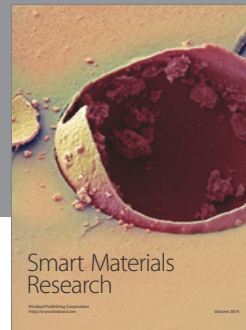
Acknowledgments

The authors would like to thank Brazilian Swiss Joint Research Programme (no. BSJRP 0112-11), PRH-ANP, CNPQ, CAPES, and UFRGS for their support.

References

- [1] J. A. Chang, M. Vithal, I. C. Baek, and S. I. Seok, "Morphological and phase evolution of TiO₂ nanocrystals prepared from peroxotitanate complex aqueous solution: influence of acetic acid," *Journal of Solid State Chemistry*, vol. 182, no. 4, pp. 749–756, 2009.
- [2] S. Da Dalt, A. K. Alves, and C. P. Bergmann, "Photocatalytic degradation of methyl orange dye in water solutions in the presence of MWCNT/TiO₂ composites," *Materials Research Bulletin*, vol. 48, no. 5, pp. 1845–1850, 2013.
- [3] H. Wang, P. Xu, and T. Wang, "Doping of Nb₂O₅ in photocatalytic nanocrystalline/nanoporous WO₃ films," *Thin Solid Films*, vol. 388, no. 1-2, pp. 68–72, 2001.
- [4] A. E. Nogueira, E. Longo, E. R. Leite, and E. R. Camargo, "Synthesis and photocatalytic properties of bismuth titanate with different structures via oxidant peroxo method (OPM)," *Journal of Colloid and Interface Science*, vol. 415, pp. 89–94, 2014.
- [5] I. Krivtsov, M. Ilkaeva, V. Avdin et al., "A hydrothermal peroxo method for preparation of highly crystalline silica-titania photocatalysts," *Journal of Colloid and Interface Science*, vol. 444, pp. 87–96, 2015.
- [6] D. Chen and X. Jiao, "Hydrothermal synthesis and characterization of Bi₄Ti₃O₁₂ powders from different precursors," *Materials Research Bulletin*, vol. 36, no. 1-2, pp. 355–363, 2001.
- [7] E. R. Camargo, J. Frantti, and M. Kakihana, "Low-temperature chemical synthesis of lead zirconate titanate (PZT) powders free from halides and organics," *Journal of Materials Chemistry*, vol. 11, no. 7, pp. 1875–1879, 2001.
- [8] E. R. Camargo and M. Kakihana, "Peroxide-based route free from halides for the synthesis of lead titanate powder," *Chemistry of Materials*, vol. 13, no. 4, pp. 1181–1184, 2001.
- [9] E. R. Camargo and M. Kakihana, "Lead hafnate (PbHfO₃) perovskite powders synthesized by the oxidant peroxo method," *Journal of the American Ceramic Society*, vol. 85, no. 8, pp. 2107–2109, 2002.
- [10] A. H. Pinto, F. L. Souza, E. Longo, E. R. Leite, and E. R. Camargo, "Structural and dielectric characterization of praseodymium-modified lead titanate ceramics synthesized by the OPM route," *Materials Chemistry and Physics*, vol. 130, no. 1-2, pp. 259–263, 2011.

- [11] H. Jiang, Y. Liu, S. Zang, J. Li, and H. Wang, "Microwave-assisted hydrothermal synthesis of Nd, N, and P tri-doped TiO₂ from TiCl₄ hydrolysis and synergetic mechanism for enhanced photoactivity under simulated sunlight irradiation," *Materials Science in Semiconductor Processing*, vol. 40, pp. 822–831, 2015.
- [12] K.-C. Huang and S.-H. Chien, "Improved visible-light-driven photocatalytic activity of rutile/titania-nanotube composites prepared by microwave-assisted hydrothermal process," *Applied Catalysis B: Environmental*, vol. 140–141, pp. 283–288, 2013.
- [13] P. Y. Qiu, N. Zhou, H. Y. Chen, C. L. Zhang, G. Gao, and D. X. Cui, "Recent advances in lanthanide-doped upconversion nanomaterials: synthesis, nanostructures and surface modification," *Nanoscale*, vol. 5, no. 23, pp. 11512–11525, 2013.
- [14] P. Kubelka and F. Munk, "Ein Beitrag zur Optik der Farbanstriche," *Zeitschrift für Technische Physik*, vol. 12, pp. 593–601, 1931.
- [15] Z.-C. Wang, J.-F. Chen, and X.-F. Hu, "Preparation of nanocrystalline TiO₂ powders at near room temperature from peroxopolytitanic acid gel," *Materials Letters*, vol. 43, no. 3, pp. 87–90, 2000.
- [16] L. J. Alemany, M. A. Bañares, E. Pardo, F. Martín-Jiménez, and J. M. Blasco, "Morphological and structural characterization of a titanium dioxide system," *Materials Characterization*, vol. 44, no. 3, pp. 271–275, 2000.
- [17] S. A. Bakar and C. Ribeiro, "An insight toward the photocatalytic activity of S doped 1-D TiO₂ nanorods prepared via novel route: as promising platform for environmental leap," *Journal of Molecular Catalysis A: Chemical*, vol. 412, pp. 78–92, 2016.
- [18] A. E. Nogueira, E. Longo, E. R. Leite, and E. R. Camargo, "Visible-light photocatalysis with bismuth titanate (Bi₁₂TiO₂₀) particles synthesized by the oxidant peroxide method (OPM)," *Ceramics International*, vol. 41, pp. 12073–12080, 2015.
- [19] J. Yu, H. Yu, B. Cheng, M. Zhou, and X. Zhao, "Enhanced photocatalytic activity of TiO₂ powder (P25) by hydrothermal treatment," *Journal of Molecular Catalysis A: Chemical*, vol. 253, no. 1–2, pp. 112–118, 2006.
- [20] B. Ohtani, Y. Ogawa, and S.-I. Nishimoto, "Photocatalytic activity of amorphous-anatase mixture of titanium(IV) oxide particles suspended in aqueous solutions," *Journal of Physical Chemistry B*, vol. 101, no. 19, pp. 3746–3752, 1997.
- [21] J. H. Jho, D. H. Kim, S.-J. Kim, and K. S. Lee, "Synthesis and photocatalytic property of a mixture of anatase and rutile TiO₂ doped with Fe by mechanical alloying process," *Journal of Alloys and Compounds*, vol. 459, no. 1–2, pp. 386–389, 2008.
- [22] H. Li, X. Shen, Y. Liu, L. Wang, J. Lei, and J. Zhang, "Facile phase control for hydrothermal synthesis of anatase-rutile TiO₂ with enhanced photocatalytic activity," *Journal of Alloys and Compounds*, vol. 646, pp. 380–386, 2015.
- [23] N.-G. Park, J. Van de Lagemaat, and A. J. Frank, "Comparison of dye-sensitized rutile and anatase-based TiO₂ solar cells," *Journal of Physical Chemistry B*, vol. 104, no. 38, pp. 8989–8994, 2000.
- [24] C. Hsu, Y. Shen, Z. Wei, D. Liu, and F. Liu, "Anatase TiO₂ nanobelts with plasmonic Au decoration exhibiting efficient charge separation and enhanced activity," *Journal of Alloys and Compounds*, vol. 613, pp. 117–121, 2014.



Hindawi

Submit your manuscripts at
<http://www.hindawi.com>

